The formation of quasi-nondiffracting focused beams with second-harmonic generation of flower Laguerre–Gaussian modes

2013 Laser Phys. 23 115405

(http://iopscience.iop.org/1555-6611/23/11/115405)

IOP PUBLISHING LASER PHYSICS
Laser Phys. **23** (2013) 115405 (6pp) doi:10.1088/1054-660X/23/11/115405

The formation of quasi-nondiffracting focused beams with second-harmonic generation of flower Laguerre–Gaussian modes

Y C Lin, K F Huang and Y F Chen

Department of Electrophysics, National Chiao Tung University, 1001 Ta Hsueh Road, Hsinchu 30050, Taiwan

E-mail: yfchen@cc.nctu.edu.tw

Received 21 August 2013, in final form 13 September 2013
Accepted for publication 16 September 2013
Published 7 October 2013
Online at stacks.iop.org/LP/23/115405

Abstract
We theoretically demonstrate that the second-harmonic generation of a flower Laguerre–Gaussian mode can be exploited to form a quasi-nondiffracting focused beam. It is verified that the product of donut Laguerre–Gaussian modes with opposite topological charges leads to the formation of the quasi-nondiffracting focused beam. The divergence of the quasi-nondiffracting focused beam is numerically confirmed to be $\sqrt{2l+1}$ times less than that of the Gaussian TEM_{00} mode with the same beam waist parameter, where l is the azimuthal index of the flower Laguerre–Gaussian mode. In an experiment, we employ a diode-pumped solid-state laser resonator with intracavity second-harmonic generation to realize the formation of the quasi-nondiffracting focused beams.

(Some figures may appear in colour only in the online journal)

1. Introduction

Focused beams have been extensively studied and applied in diverse fields. Remarkable examples are in optical tweezers [1, 2], lithography [3], optical data storage [4], optical interconnects [5], biophotonics [6], and optical coherence tomography [7]. Gaussian TEM_{00} modes have been the prevalent ones since they can be emitted by most laser cavities. In recent decades, the zeroth-order Bessel beam has become an alternative method for the Gaussian TEM_{00} mode in related topics on beam focusing [5–9]. Unlike the conventional Gaussian modes with the beam divergence of the order of the Rayleigh range, Bessel beams have gained attention because of their inherent characteristic of nondiffraction or non-spreading [10–12]. This fascinating feature has led to progressive developments such as in the alignment of rod-like samples, stacking and manipulation of multiple spheres, and guiding of spheres along the extended line focus of a Bessel beam [9]. The finding of such a diffraction-free solution to the Bessel beam [13] has not only stimulated a great number of theoretical and experimental studies but has also paved the way to the discovery of other intriguing nondiffracting focused beams, including the Airy beam [14, 15].

In addition to the Bessel beam, the Laguerre–Gaussian (LG) modes $\Psi_{p,\pm l}$ are also solutions to the Helmholtz equation in cylindrical coordinates, where p is the radial index, $\pm l$ is the azimuthal index, and the sign $\pm$ signifies the opposite topological charges. The spatial distributions of high-order $\Psi_{p,0}$ modes are similar to those of Bessel beams which possess a sharp central peak with inherent nondiffracting properties [16, 17]. In contrast, the flower LG mode [18–24], consisting of $\Psi_{0,l}$ and $\Psi_{0,-l}$ modes, possesses a null at the beam center. The flower LG modes have been experimentally explored in a large-aperture CO_2 laser [18], optically pumped [21] and electrically pumped [22] vertical-cavity surface emitting semiconductor lasers (VCSELs), and a solid-state laser cavity with a

nonlinear medium [19, 23, 24]. It has been shown that the attractive features of the flower LG modes lead to rich studies in pattern formation [19, 23, 24] and recent research on the generation of two-dimensional optical vortex arrays [20].

In this work we first show that the second-harmonic generation (SHG) of a flower LG mode can give rise to the formation of a nondiffracting focused beam. We verify that the SHG of the flower LG mode can yield a cross term $\Psi_{0,l}\Psi_{0,-l}$. With the re-projection scheme, the cross term $\Psi_{0,l}\Psi_{0,-l}$ can be analytically expressed to be a coherent superposition of a set of $\Psi_{p,0}$ modes with $0 \le p \le l$. The derived expression clearly reveals that the distinct Gouy phases between the different $\Psi_{p,0}$ modes lead to the formation of a bright central maximum. The bright central beam displays a nondiffracting feature with the divergence numerically calculated to be $\sqrt{2l+1}$ times less than that of the Gaussian TEM_{00} mode with the same beam waist parameter. Finally, we use a diode-pumped solid-state laser cavity with intracavity SHG to experimentally confirm the formation of the quasi-nondiffracting focused beam. Here, the term 'quasi-nondiffracting' is used to distinguish a nearly nondiffracting beam that actually diffracts during propagation from an ideal diffraction-free one.

2. Theoretical analysis

Under the paraxial approximation, the traveling LG mode $\Psi_{p,\pm l}$ with the wavenumber k and the beam waist w_o is given by [25]

$$\begin{aligned}\Psi_{p,\pm l}(r,\phi,z;k,w_o) = (-1)^p \frac{N_{p,l}}{w(z)}\left(\frac{\sqrt{2}r}{w(z)}\right)^l L_p^l\left(\frac{2r^2}{w(z)^2}\right)\\ \times \exp(\pm \mathrm{i}\, l\phi)\exp\left(-\frac{r^2}{w(z)^2}\right)\\ \times \exp(\mathrm{i}\gamma k z)\\ \times \exp[\mathrm{i}\,(2p+l+1)\,\theta_{\mathrm{G}}(z)],\end{aligned} \tag{1}$$

where $w(z) = w_o\sqrt{1+(z/z_{\mathrm{R}})^2}$ is the spot size at z, w_o is the beam radius at $z=0$, $z_{\mathrm{R}} = k w_o^2/2$ is the Rayleigh range, $\gamma = 1 + r^2/[2(z^2+z_{\mathrm{R}}^2)]$, $\theta_{\mathrm{G}}(z) = \tan^{-1}(z/z_{\mathrm{R}})$ is the Gouy phase, $N_{p,l} = \sqrt{2p!/(1+\delta_{0,l})\pi(l+p)!}$ is the constant for normalization, where $\delta_{0,l} = 1$ for $l = 0$, and $L_p^l(\cdot)$ is the associated Laguerre polynomial of integer indices l and p in the azimuthal and radial directions, respectively. The sign $\pm$ in the representation $\Psi_{p,\pm l}$ indicates opposite topological charges. The standing wave LG mode is the coherent superposition of a pair of traveling wave LG modes with equal but opposite topological charges. In general, the basis for the standing wave LG modes is expressed as

$$\Psi_{p,l}^c = \left(\Psi_{p,+l} + \Psi_{p,-l}\right)/\sqrt{2} \tag{2a}$$

and

$$\Psi_{p,l}^s = \left(\Psi_{p,+l} - \Psi_{p,-l}\right)/\sqrt{2}\mathrm{i}, \tag{2b}$$

where the subscripts c and s are employed to express wavefunctions with azimuthal distributions of $\cos(l\phi)$ and $\sin(l\phi)$, respectively. Unlike the traveling wave LG mode, the standing wave LG mode of $l \neq 0$ possesses no net orbital angular momentum. For $p = 0$, the traveling wave LG mode $\Psi_{p,\pm l}$ exhibits a simple donut structure, whereas the standing wave LG mode $\Psi_{p,l}^c$ or $\Psi_{p,l}^s$ displays a flower structure.

Next we consider that the flower LG mode is used as the fundamental wave for the second-harmonic process. Under the non-depletion approximation, the amplitude of the frequency-doubled field is proportional to the square of the fundamental field [26]. Furthermore, the second-harmonic process is generally implemented with focusing of the fundamental wave into the nonlinear crystal; namely, the generation of the second-harmonic wave is near the region of the beam waist, $z = 0$. Therefore, the second-harmonic wave for the fundamental flower LG mode with the wavenumber k_1 and the beam waist w_{1o} at $z = 0$ is given by

$$\Phi(r,\phi,0) = \eta[\Psi_{0,l}^c(r,\phi,0;k_1,w_{1o})]^2, \tag{3}$$

where η is a constant related to the conversion efficiency in the second-harmonic process. Here, we consider the case of the cosine LG mode for convenience. Substituting equation (2*a*) into equation (3), the second-harmonic wave $\Phi(r,\phi,0)$ at the beam waist can be expressed as

$$\begin{aligned}\Phi(r,\phi,0) = \frac{\eta}{2}\{&[\Psi_{0,+l}(r,\phi,0;k_1,w_{1o})]^2\\ &+ [\Psi_{0,-l}(r,\phi,0;k_1,w_{1o})]^2\\ &+ 2\Psi_{0,+l}(r,\phi,0;k_1,w_{1o})\\ &\times \Psi_{0,-l}(r,\phi,0;k_1,w_{1o})\}.\end{aligned} \tag{4}$$

With the given distribution $\Phi(r,\phi,0)$ evaluated at $z = 0$, we can then derive the z-dependent expression of the second-harmonic wave $\Phi(r,\phi,z)$ in terms of the Fresnel diffraction integral [25],

$$\begin{aligned}\Phi(r,\phi,z) = \frac{k_2}{\mathrm{i}\,2\pi\, z}\exp\left(\mathrm{i}\frac{2\pi z}{k_2}\right)\int_0^\infty\int_0^{2\pi}\Phi(r,\phi,0)\\ \times \exp\left(\mathrm{i}\,\frac{k_2\, r^2}{2z}\right) r\,\mathrm{d}\phi\,\mathrm{d}r.\end{aligned} \tag{5}$$

To analytically manifest the z-dependence of the second-harmonic wave $\Phi(r,\phi,z)$ with a closed form, the wavefunction in equation (4) needs to be expanded with the LG modes and the parameters need to be changed from k_1 and w_{1o} for the fundamental wave to k_2 and w_{2o} for the second-harmonic wave, where $k_2 = 2k_1$ and $w_{2o}^2 = w_{1o}^2/2$. With equation (1), it can be verified that

$$\begin{aligned}\left[\Psi_{0,\pm l}(r,\phi,0;k_1,w_{1o})\right]^2 = \frac{\sqrt{(2l)!}}{\sqrt{2\pi}\,2^l\, l! w_{2o}}\\ \times \Psi_{0,\pm 2l}(r,\phi,0;k_2,w_{2o}).\end{aligned} \tag{6}$$

Equation (6) indicates that the SHG of the donut LG mode $\Psi_{0,\pm l}$ directly leads the orbital angular momentum per photon to double from $l\hbar$ to $2l\hbar$. The corresponding experimental realization was popularized in previous work by Dholakia *et al* [27]. On the other hand, the cross term $\Psi_{0,+l}(r,\phi,0;k_1,w_{1o})\Psi_{0,-l}(r,\phi,0;k_1,w_{1o})$ in equation (4)

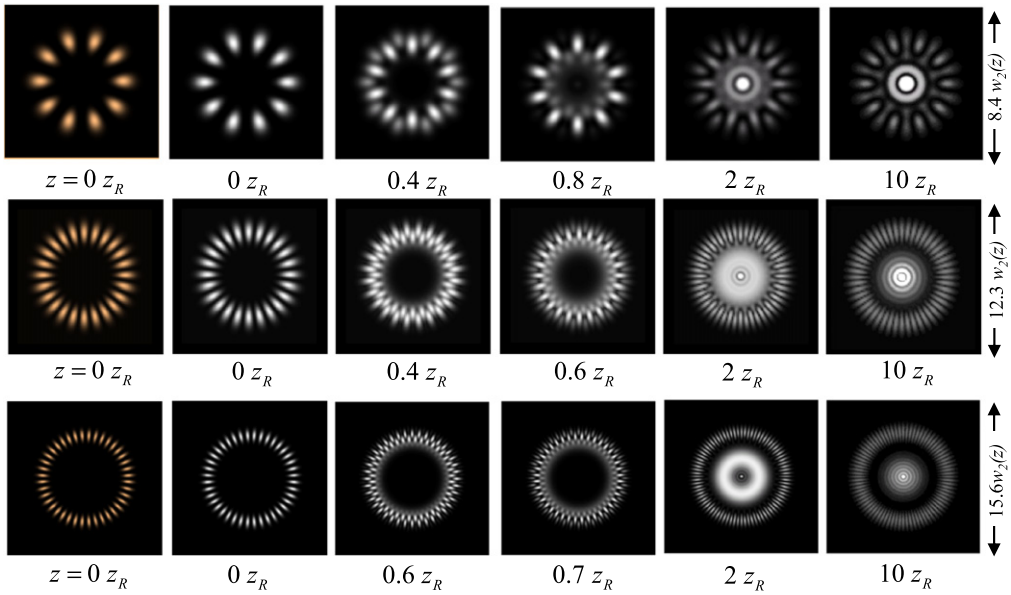

Figure 1. Theoretical simulations for the fundamental flower LG modes $\left|\Psi^c_{0,l}(r,\phi,0;k_1,w_{1o})\right|^2$ at the beam waist, $z = 0$ (first column), and their second-harmonic counterparts $|\Phi(r,\phi,z)|^2$ from $z = 0$ to $10z_R$. First row: $l = 5$, second row: $l = 12$, third row: $l = 20$.

can be expanded with the expression [28]

$$x^l = l! \sum_{n=0}^{l} C^l_n \,(-1)^n \, L_n\,(x)\,, \tag{7}$$

where $C^l_n = l!/[n!(l-n)!]$ is the binomial coefficient. With equation (7), the cross term can be expressed as

$$\Psi_{0,+l}\,(r,\phi,0;k_1,w_{1o})\,\Psi_{0,-l}\,(r,\phi,0;k_1,w_{1o}) = \frac{1}{\sqrt{\pi}\,2^l w_{2o}} \sum_{n=0}^{l} C^l_n \Psi_{n,0}\,(r,\phi,0;k_2,w_{2o})\,. \tag{8}$$

It is clear that the multiplication of the LG modes with opposite topological charges is derived to be the coherent superposition of a set of LG modes $\Psi_{n,0}(r,\phi,0;k_2,w_{2o})$, as shown in equation (8). Although all the LG modes $\Psi_{n,0}(r,\phi,0;k_2,w_{2o})$ in equation (8) possess the maximum intensity at the beam center, $r = 0$, it is worth noting that the interference leads the superposed wave $\sum_{n=0}^{l} C^l_n \Psi_{n,0}(r,\phi,0;k_2,w_{2o})$ to display a null at $r = 0$. Substituting equations (6) and (8) into equation (4), we can obtain

$$\Phi(r,\phi,0) = \frac{\eta}{2^l\sqrt{\pi}\,w_{2o}}\left[\frac{\sqrt{(2l)!}}{2\,(l!)}\Psi^c_{0,2l}\,(r,\phi,0;k_2,w_{2o}) + \sum_{n=0}^{l} C^l_n \Psi_{n,0}\,(r,\phi,0;k_2,w_{2o})\right]. \tag{9}$$

The well-known propagation characteristics of the LG modes $\Psi_{p,\pm l}(r,\phi,z;k_2,w_o)$ in equation (1) and $\Psi^c_{p,l}(r,\phi,z;k_2,w_o)$ in equation (2*a*) can be used to predict the amplitude function for $\Phi(r,\phi,z)$ at any cross section z via the Fresnel diffraction integral. Substituting the expansion in equation (9) for $\Phi(r,\phi,0)$ in equation (5), the z-dependence of the second-harmonic wave can thus be given by

$$\Phi(r,\phi,z) = \frac{\eta}{2^l\sqrt{\pi}\,w_{2o}}\left[\frac{\sqrt{(2l)!}}{2\,(l!)}\Psi^c_{0,2l}\,(r,\phi,z;k_2,w_{2o}) + \sum_{n=0}^{l} C^l_n \Psi_{n,0}\,(r,\phi,z;k_2,w_{2o})\right]. \tag{10}$$

From equation (1), it can be understood that the variations of the Gouy phases in the propagation are not the same for the LG modes $\Psi_{n,0}(r,\phi,z;k_2,w_{2o})$ with different orders n. As a consequence, even though the superposed wave $\sum_{n=0}^{l} C^l_n \Psi_{n,0}(r,\phi,z;k_2,w_{2o})$ at the beam waist, $z = 0$, displays a null at the beam center, $r = 0$, the influence of the Gouy phase leads to an intriguing phenomenon that the second-harmonic wave $\Phi(r,\phi,z)$ in the propagation starts to display a central maximum. To be brief, the cross term $\Psi_{0,+l}\Psi_{0,-l}$ shown in equation (8) results in the superposed term $\sum_{n=0}^{l} C^l_n \Psi_{n,0}(r,\phi,z;k_2,w_{2o})$ which forms a focused beam in the propagation.

In figure 1, we theoretically present the intensity profiles of the fundamental flower LG modes $|\Psi^c_{0,l}(r,\phi,0;k_1,w_{1o})|^2$ at the beam waist, $z = 0$, and their second-harmonic counterparts $|\Phi(r,\phi,z)|^2$ at different longitudinal positions from $z = 0$ to $10z_R$. It can be seen that the second-harmonic LG modes $|\Phi(r,\phi,0)|^2$ display the same flower structures as the fundamental LG modes $|\Psi^c_{0,l}(r,\phi,0;k_1,w_{1o})|^2$ with a null at the beam center. From $z = 0$ to $10z_R$, we observe the formation of bright central maxima for the second-harmonic fields $|\Phi(r,\phi,z)|^2$ due to the interference of the $\Psi_{n,0}(r,\phi,z;k_2,w_{2o})$ modes with different Gouy phases. For a higher-order $|\Phi(r,\phi,z)|^2$ field such as $l = 20$ in the third row, a concentric-ringed structure is developed around the bright central maximum owing to the interference of some higher-order $\Psi_{n,0}(r,\phi,z;k_2,w_{2o})$

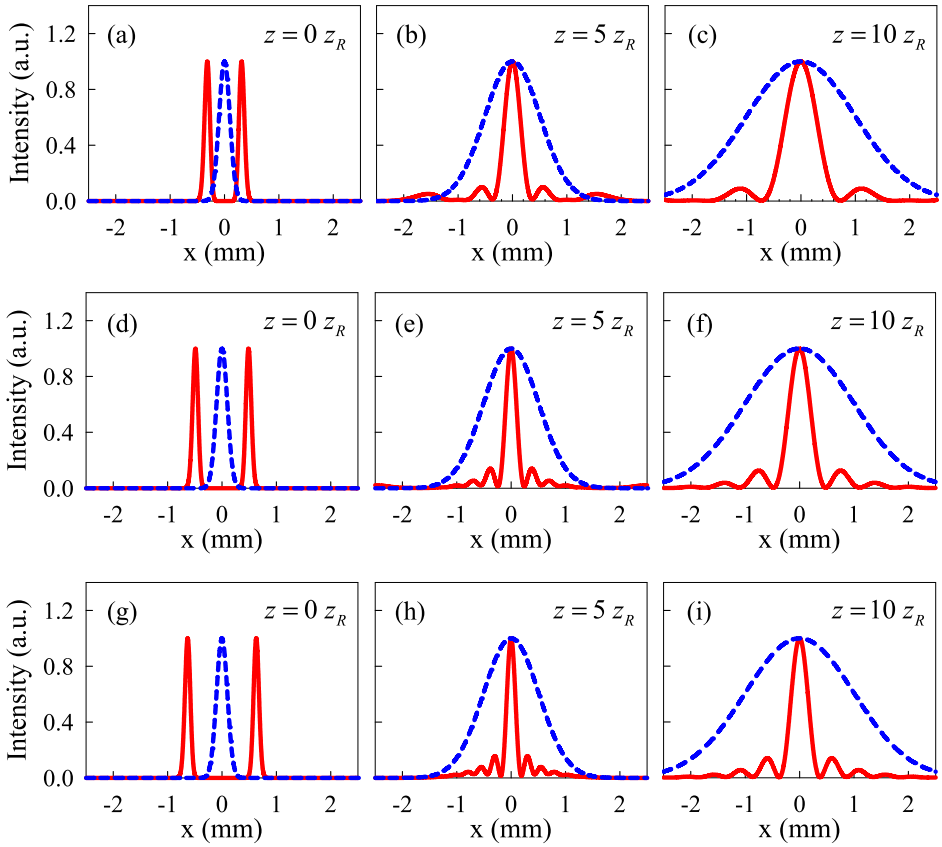

Figure 2. The intensity distribution of the cross sections for the frequency-doubled beams $|\Phi(r, \phi, z)|^2$ (solid line) and the Gaussian TEM_{00} modes $|\Psi_{0,0}(r, \phi, z;\ k_2, w_{2o})|^2$ (dashed line) at $z = 0, 5z_R$, and $10z_R$ with (a)–(c) $l = 5$, (d)–(f) $l = 12$, (g)–(i) $l = 20$.

modes. Moreover, the influence of the superposed state $\sum_{n=0}^{l} C_n^l \Psi_{n,0}(r, \phi, z; k_2, w_{2o})$ on the propagation-invariant term $\Psi^c_{0,2l}(r, \phi, z; k_2, w_{2o})$ in equation (10) is shown in figure 1, where the flower structures evolve with their azimuthal indices transforming from l to $2l$ along the longitudinal direction.

Figure 2 illustrates the intensity distribution of the cross sections for the second-harmonic waves $|\Phi(r, \phi, z)|^2$ and the Gaussian TEM_{00} mode $|\Psi_{0,0}(r, \phi, z; k_2, w_{2o})|^2$ at $z = 0z_R, z = 5z_R$ and $z = 10z_R$ to clearly reveal the quasi-nondiffracting properties of the central lobes. It can be seen that the divergence of the central peaks is directly decided by the orders l of the flower LG modes $\Psi^c_{0,l}(r, \phi, 0; k_1, w_{1o})$. The divergence of the central peak for the second-harmonic wave $|\Phi(r, \phi, z)|^2$ is qualitatively estimated to be $\sqrt{2l+1}$ times less than that of the Gaussian TEM_{00} mode $|\Psi_{0,0}(r, \phi, z; k_2, w_{2o})|^2$ with the same beam waist parameter. As the order l of the flower LG mode $\Psi^c_{0,l}(r, \phi, 0; k_1, w_{1o})$ gets higher, the divergence of the bright center for the second-harmonic wave $|\Phi(r, \phi, z)|^2$ becomes smaller. The central parts of the high-order $|\Phi(r, \phi, z)|^2$ modes conserve their profiles through several Rayleigh ranges without obvious divergence, showing the quasi-nondiffracting properties. Previous works [16, 17] have shown that the central lobes of high-order $\Psi_{n,0}(r, \phi, z; k, w_o)$ modes are characterized by their nondiffracting features. In this investigation we validate that the bright center arising from the coherent superposition of the group of $\Psi_{n,0}(r, \phi, z; k_2, w_{2o})$ modes can exhibit the feature of a quasi-nondiffracting beam. The nondiffracting focused phenomena of optical waves have great importance for applications such as optical trapping and optical manufacturing. Therefore, it might be useful to generate such second-harmonic focused beams characterized by their inherent quasi-nondiffracting features through the SHG. In the following, we exploit a diode-pumped solid-state laser with intracavity SHG to experimentally confirm the formation of the quasi-nondiffracting focused beam.

3. Experimental realization

The schematic diagram for the experimental setup of a diode-pumped Nd:YVO_4 laser with a KTP crystal as an intracavity SHG medium is illustrated in figure 3. The experimental configuration was designed for SHG at 532 nm from a fundamental wavelength of 1064 nm. The laser medium was an a-cut 2.0 at.% Nd:YVO_4 crystal with a length of 2 mm and a cross section of 10×10 mm^2. The SHG medium was a 10-mm-long KTP crystal with a cutting angle ($\theta = 90°$ and $\varphi = 23.5°$) to satisfy the type II SHG phase matching condition. Both sides of the Nd:YVO_4 and KTP crystals were coated for antireflection at 1064 nm ($R < 0.2\%$). In addition, they were wrapped with indium foil and mounted in a water-cooled copper block. The front mirror was a 250 mm radius-of-curvature concave mirror with

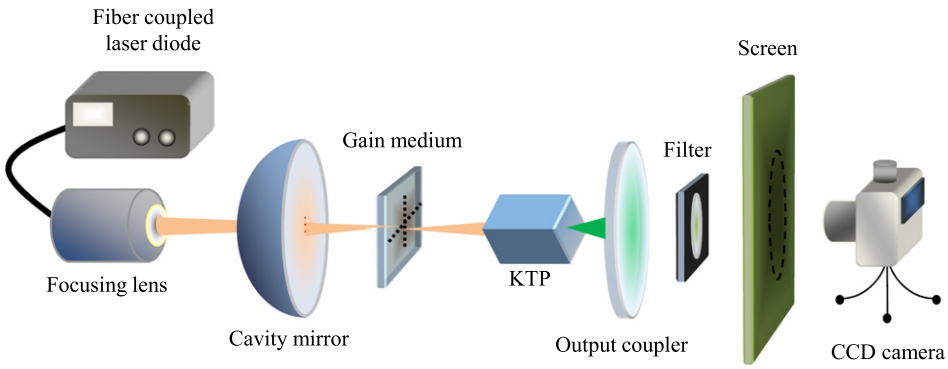

Figure 3. The experimental setup of the diode-pumped solid-state laser with intracavity SHG.

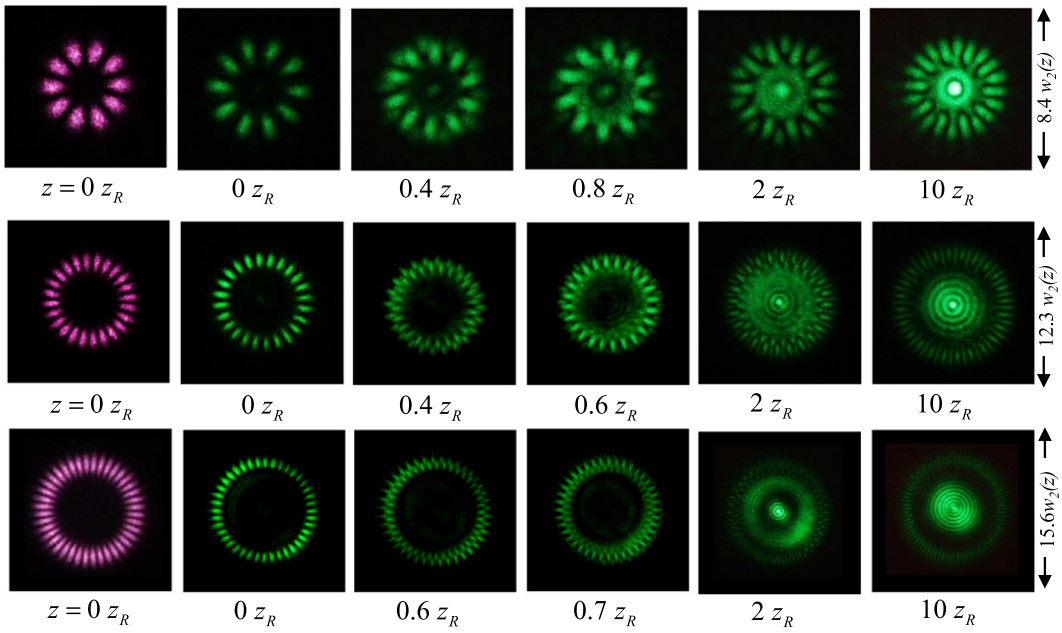

Figure 4. The observed transverse intensity profiles of the fundamental flower LG modes $|\Psi^c_{0,l}(r, \phi, 0; k_1, w_{1o})|^2$ at $z = 0$ (first column) and their second-harmonic counterparts $|\Phi(r, \phi, z)|^2$ from $z = 0$ to $10z_R$. First row: $l = 5$, second row: $l = 12$, third row: $l = 20$.

antireflection ($R < 0.2\%$) coating at 808 nm on the entrance surface ($R < 0.2\%$) and high-reflection coating at 1064 nm ($R > 99.8\%$) and 532 nm ($R > 99\%$) on the other surface. The output coupler was a flat mirror with partial-reflection coating at 1064 nm ($R = 98\%$) and high-transmission coating at 532 nm ($T > 85\%$). The pump source was an 808 nm fiber-coupled laser diode with a pump core of 100 μm in radius, a numerical aperture of 0.16, and a maximum output power of 1 W. A focusing lens with a focal length of 25 mm and 85% coupling efficiency was used to reimage the pump beam into the laser medium.

To generate the high-order flower LG modes of different orders, we employed a donut-shaped pump profile and defocused a standard fiber-coupled diode [23]. At the focal plane, the profile for a multi-mode fiber-coupled diode laser beam passing through a focusing lens is like a top-hat distribution; however, away from the focal plane it is like a donut-shaped distribution. Based on this property, we defocused a standard fiber-coupled diode to obtain a good overlap with a high-order flower $LG_{0,l}$ mode and generate it purely. Flower LG modes of varying orders correspond to differing sizes of the pump profiles. The pump spot sizes were controlled to be 50–200 μm. The overall cavity length was nearly 80 mm. According to the experimental scheme, the beam radius of the fundamental TEM_{00} mode can be calculated to be around 141 μm. The difference of the beam radius between adjacent flower LG modes is of the order of 40 μm. With a pump power of 800 mW, the average output power is found to be 80 mW for the second-harmonic TEM_{00} mode. The conversion efficiency for the second-harmonic TEM_{00} mode from the diode laser incident power to the SHG output is about 12%. However, for the second-harmonic standing wave LG mode of $l = 12$, the average output power is measured to be 0.84 mW with a pump power of 745 mW. To scale up the output power, the laser diode can be replaced with a high-power one. In this case, a less Nd-doped laser medium should be employed to reduce the severe thermal issues owing to the concentration quenching. Moreover, filters

placed after the laser cavity allow either the fundamental or the second-harmonic wave to be chosen and projected onto a screen. The projected patterns were observed through a CCD camera. Figure 4 displays the experimental results for the formation of the quasi-nondiffracting focused beams corresponding to figure 1. The experimental tomographic transverse patterns show good agreement with the theoretical simulations in figure 1. This investigation confirms that a nondiffracting focused beam can be experimentally realized through the intracavity SHG of flower LG modes.

4. Conclusions

In summary, we have theoretically demonstrated that the generation of quasi-nondiffracting focused beams can be realized through the nonlinear SHG of flower LG modes. The formation of the quasi-nondiffracting focused beam has been analytically verified to result from the cross term $\Psi_{0,l}\Psi_{0,-l}$. We have further confirmed that the divergence of the nondiffracting focused beam is approximately $\sqrt{2l+1}$ times less than that of the Gaussian TEM_{00} mode with the same beam waist parameter. Finally, we have employed a diode-pumped solid-state laser cavity to experimentally generate a quasi-nondiffracting focused beam via the intracavity SHG of flower LG modes.

Acknowledgment

The authors acknowledge the National Science Council of Taiwan (NSCT) for their financial support of this research under contract NSC-100-2628-M-009-001-MY3.

References

[1] Ashkin A, Dziedzic J M, Bjorkholm J E and Chu S 1986 *Opt. Lett.* **11** 288
[2] Ashkin A, Dziedzic J M and Yamane T 1987 *Nature* **330** 769
[3] Takashi I and Shinji O 2000 *Nature* **406** 1027
[4] Strickler J H and Webb W W 2002 *Opt. Lett.* **16** 1780
[5] Yu C, Wang M R, Varela A J and Chen B 2000 *Opt. Commun.* **177** 369
[6] Tsampoula X, Garcés-Chávez V, Comrie M, Stevenson D J, Agate B, Brown C T A, Gunn-Moore F and Dholakia K 2007 *Appl. Phys. Lett.* **91** 053902
[7] Ding Z, Ren H, Zhao Y, Nelson J S and Chen Z 2002 *Opt. Lett.* **27** 243
[8] Garcés-Chávez V, McGloin D, Melville H, Sibbett W and Dholakia K 2002 *Nature* **419** 145
[9] Arlt J, Garces-Chavez V, Sibbett W and Dholakia K 2001 *Opt. Commun.* **197** 239
[10] Durnin J, Miceli J J and Eberly J H 1987 *Phys. Rev. Lett.* **58** 1499
[11] McGloin D and Dholakia K 2005 *Contemp. Phys.* **46** 15
[12] Bouchal Z, Wagner J and Chlup M 1998 *Opt. Commun.* **151** 207
[13] Durnin J 1987 *J. Opt. Soc. Am.* A **4** 651
[14] Siviloglou G A, Broky J, Dogariu A and Christodoulides D N 2007 *Phys. Rev. Lett.* **99** 213901
[15] Zhang P, Prakash J, Zhang Z, Mills M S, Efremidis N K, Christodoulides D N and Chen Z 2011 *Opt. Lett.* **36** 2883
[16] Flood C J, Giuliani G and van Driel H M 1990 *Opt. Lett.* **15** 215
[17] Senatsky Y, Bisson J-F, Li J, Shirakawa A, Thirugnanasambandam M and Ueda K-i 2012 *Opt. Rev.* **19** 201
[18] Green C, Mindlin G B, D'Angelo E J, Solari H G and Tredicce J R 1990 *Phys. Rev. Lett.* **65** 3124
[19] Grynberg G, Maitre A and Petrossian A 1994 *Phys. Rev. Lett.* **72** 2378
[20] Lin Y C, Lu T H, Huang K F and Chen Y F 2011 *Opt. Express* **19** 10293
[21] Pereira S F, Willemsen M B, van Exter M P and Woerdman J P 1998 *Appl. Phys. Lett.* **73** 2239
[22] Deng Q, Deng H and Deppe D G 1997 *Opt. Lett.* **22** 463
[23] Chen Y F and Lan Y P 2001 *Phys. Rev.* A **63** 063807
[24] Ito A, Kozawa Y and Sato S 2010 *J. Opt. Soc. Am.* A **27** 2072
[25] Siegman A E 1986 *Lasers* (Mill Valley, CA: University Science Books)
[26] He G S and Liu S H 1990 *Physics of Nonlinear Optics* (Singapore: World Scientific)
[27] Dholakia K, Simpson N B and Padgett M J 1996 *Phys. Rev.* A **54** R3742
[28] Lebedev N N and Silverman R A 1965 *Special Functions and their Applications* (Englewood Cliffs, NJ: Prentice-Hall)